Journal for ImmunoTherapy of Cancer

Inhibition of stromal MAOA leading activation of WNT5A enhance prostate cancer immunotherapy by involving the transition of cancer-associated fibroblasts

Zhite Zhao,[1,2] Yaohua Hu,[2] Hui Li,[2] Tong Lu ,[1] Xinglin He,[1] Yifan Ma,[2] Minli Huang,[2] Mengyao Li,[2] Lijun Yang,[1] Changhong Shi [3,4]

To cite: Zhao Z, Hu Y, Li H, *et al*. Inhibition of stromal MAOA leading activation of WNT5A enhance prostate cancer immunotherapy by involving the transition of cancer-associated fibroblasts. *Journal for ImmunoTherapy of Cancer* 2025;**13**:e010555. doi:10.1136/jitc-2024-010555

► Additional supplemental material is published online only. To view, please visit the journal online (https://doi.org/10.1136/jitc-2024-010555).

Accepted 12 March 2025

[1]Department of Urology, Xijing Hospital, Fourth Military Medical University, Xi'an, Shaanxi, China
[2]Division of Cancer Biology, Laboratory Animal Center, Fourth Military Medical University, Xi'an, Shaanxi, China
[3]Fourth Military Medical University, Xi'an, Shaanxi, China
[4]State Key Laboratory of Holistic Integrative Management of Gastrointestinal Cancers, Xi'an, Shaanxi, China

Correspondence to
Dr Changhong Shi;
changhong@fmmu.edu.cn

ABSTRACT

Background The interaction between stromal cells and the tumor immune microenvironment (TIME) is acknowledged as a critical driver in the progression of prostate cancer (PCa). Monoamine oxidase A (MAOA), a mitochondrial enzyme that catalyzes the degradation of monoamine neurotransmitters and dietary amines, has been linked to the promotion of prostate tumorigenesis, particularly when upregulated in stromal cells. However, the detailed mechanisms of MAOA's interaction with TIME have not been fully elucidated.

Methods We reanalyzed a single-cell sequencing dataset to evaluate the role of MAOA in the stroma, verify the impact of stromal MAOA alterations on $CD8^+$ T cell responses by co-culturing stromal cells and immune cells in vitro. Furthermore, C57BL/6J mouse subcutaneous transplant tumor models and dual humanized mouse models were established to investigate the function of MAOA in vivo and the potential of its inhibitors for immunotherapy.

Results Our study demonstrates that inhibiting MAOA in stromal cells facilitates the conversion of myofibroblastic cancer-associated fibroblasts (myCAFs), thereby improving the immunosuppressive environment of PCa. The strategic combination of MAOA inhibition with immune checkpoint inhibitors elicits a synergistic antitumor effect. Specifically, MAOA inhibition in stromal cells leads to increased production of WNT5A, which subsequently activates the cytotoxic capacity of $CD8^+$ T cells through the Ca^{2+}-NFATC1 signaling pathway.

Conclusions Our findings highlight the critical role of MAOA in modulating cancer-associated fibroblasts within the PCa immune microenvironment, presenting a novel therapeutic strategy to augment the efficacy of immunotherapy for PCa.

INTRODUCTION

Prostate cancer (PCa) is one of the major threats to men's health worldwide. According to the latest cancer statistics, PCa has become the most common cancer among men and

WHAT IS ALREADY KNOWN ON THIS TOPIC

⇒ In the tumor microenvironment (TME), stromal cells play a crucial role. They not only provide structural support for tumor cells but also participate in the development and immune evasion of tumors by secreting various cytokines and enzymatic molecules. Monoamine oxidase A (MAOA) also plays a complex role in this process. Within the TME, MAOA may affect the progression of prostate cancer (PCa) by influencing the interactions between tumor cells and stromal cells. However, the precise mechanisms by which MAOA in the stroma regulate immune cell functions have not yet been elucidated.

WHAT THIS STUDY ADDS

⇒ In our study, single-cell sequencing technology revealed the significant role of MAOA in the transition of myCAFs to modulate immune responses. The study found that inhibiting MAOA in the stroma of PCa promotes the production of the WNT5A secretory protein. This WNT5A, secreted by cancer-associated fibroblasts, significantly enhances the antitumor immune effect of $CD8^+$ T cells through the Ca^{2+}-NFATC1 signaling pathway. Moreover, combining therapy targeting stromal MAOA with immune checkpoint inhibitors (ICIs) shows synergistic antitumor effects.

HOW THIS STUDY MIGHT AFFECT RESEARCH, PRACTICE OR POLICY

⇒ This study reveals that inhibiting MAOA in stromal cells can significantly enhance the secretion of WNT5A. This increase in WNT5A activates the Ca^{2+}-NFATC1 signaling pathway in $CD8^+$ T cells, thereby strengthening the antitumor immune response. This discovery elucidates the mechanism by which stromal MAOA modulates the response of $CD8^+$ T cells. Furthermore, the combined therapeutic strategy of MAOA inhibitors with ICIs may not only improve treatment efficacy and reduce side effects but also expand the therapeutic options available to patients.

has risen to become the second leading cause of cancer-related deaths in males.[1] Although early-stage PCa can be effectively controlled through surgery or radiotherapy, treatment options for advanced stages, especially metastatic castration-resistant prostate cancer (CRPC), are limited and the prognosis is poor.[2] Immunotherapy, particularly immune checkpoint inhibitors (ICIs) and CAR T-cell therapy, has demonstrated remarkable potential in treating certain malignant tumors.[3–5] However, its application in PCa faces obstacles such as the tumor's immune evasion strategies and the lack of effective predictive biomarkers. These challenges underscore the need for further investigation into immunotherapy's potential in PCa.[6–8] The tumor microenvironment (TME) plays a critical role in PCa development and progression. Inappropriate activation of the stroma potentiates the growth and transformation of epithelial tumor cells.[9 10] Recent research on the TME has shed light on the role of stromal cells like cancer-associated fibroblasts (CAFs) in modulating immune responses and fueling tumor growth.[11–13] CAFs can facilitate tumor immune evasion by secreting an array of proteins, cytokines, and chemokines, which are primarily associated with ICI therapy resistance.[14] Thus, CAFs are critical components of the immunologically "cold" TME and are considered a promising target to enhance the immunotherapy response.

Monoamine oxidase A (MAOA) is a mitochondrial enzyme that can degrade neurotransmitters in the brain and influence mood and behavior. [15]With the progress of research, the role of MAOA in tumors is gaining attention, as it can promote PCa growth, metastasis, stemness, and therapeutic resistance.[16–19] This promotion is primarily through increasing oxidative stress, enhancing hypoxia, inducing epithelial–mesenchymal transition, and activating multiple signaling pathways regulated by the downstream transcription factor Twist1. Moreover, MAOA has been implicated in the TME of PCa, with upregulated expression in stromal cells promoting prostate tumorigenesis. Related experiments demonstrated that the activity of tumor-infiltrating T cells is related to the expression of MAOA in cells. MAOA inhibitors can activate $CD8^+$ T cells by upregulating the serotonin (5-HT) autocrine pathway of these cells, significantly suppressing tumor growth. Preclinical mouse syngeneic and human xenograft tumor models have shown antitumor effects of MAOA inhibitors, especially when combined with anti-programmed cell death protein-1 (PD-1) therapy.[20] This suggests that MAOA inhibition holds therapeutic promise for PCa. However, the interplay between stromal MAOA and the immune microenvironment of PCa requires further clarification.

In this study, we used single-cell sequencing in PCa to identify MAOA's involvement in the conversion of myofibroblastic cancer-associated fibroblasts (myCAFs) to modulate immune responses. The role of stromal MAOA in PCa development and its influence on the immunosuppressive TME were further explored. By elucidating these mechanisms, we aim to provide insights into the potential of targeting stromal MAOA in combination with immunotherapy as a novel strategy for treating PCa.

MATERIALS AND METHODS

Human samples

Human PCa samples were obtained from Xijing Hospital of the Fourth Military Medical University. The human PCa tissue microarray (TMA) was purchased from WEIAO BIO (#ZL-PRC1601; Shanghai, China).

Cell lines and cell culture

Human PCa cell lines (PC3, DU145, C42, 22RV1), mouse PCa cell lines (RM-1, Tramp-C1), Human prostate stromal myofibroblast (WPMY-1) and Human leukemia cell line (JURKAT) were obtained from the American Type Culture Collection (Manassas, Virginia, USA) and cultured in Roswell Park Memorial Institute 1640 and Dulbecco's Modified Eagle's Medium supplemented with 10% fetal bovine serum (Gibco). Human primary PCa stromal cells (H-PrSC) were isolated from tumor samples obtained from patients with PCa at the Xijing Hospital of the Fourth Military Medical University. Mouse prostate stromal cells (M-PrSC) were isolated from the prostate tissues of 8 to 12 week-old C57BL/6 mice. Stromal cells were cultured in iCell fibroblast medium (iCell Bioscience Shanghai, China PriMed-iCell-003). Human peripheral blood mononuclear cells (PBMCs) were derived from fresh blood of patients with PCa and normal blood donors. All cells were cultured at 37°C in a 5% CO_2 environment. In addition to the aforementioned culture media and serum, reagents designated as BOX5 TFA (MedChemExpress, HY-123071A) N-acetylcysteine (NAC) (Beyotime, S0077), and hydrogen peroxide (H_2O_2) (DAMAO, 7722-84-1) were incorporated into the cell culture program to study cellular experiments.

PCa organoid model

Fresh human PCa tissues and matched fresh blood were obtained from Xijing Hospital of the Fourth Military Medical University. The tissues were cut into small pieces and cultured in a 15 mL centrifuge tube containing digestive liquid (2.5 mg/mL Type II Collagenase and 10 µM Y-27632 in basal medium) for 1 hour. The digested products were filtered through a 70 µm filter and the supernatant was removed. Cells were cultured with 30 µL of Matrigel in a 24-well plate (1×10^5 cells/well) for 15 min. After the Matrigel solidified, 500 µL of organoid culture medium was added to construct the organoid model. Fresh blood was used to obtain PBMCs. 2×10^4 WPMY-1 cells per well were added and co-cultured with the organoids for 7 days. After 7 days, 2×10^5 PBMCs that had been activated with CD3 (1 µg/mL) /CD28 (1 µg/mL) (Thermo Fisher, 16-0037-81/16-0289-81) for 1 day were added to each well and further cultured for 3 days to assess whether MAOA in the stromal cells depends on the immune influence on the viability of the organoids.

Bioinformatics analysis

Tumor IMmune Estimation Resource (TIMER) (http://cistrome.org/TIMER/) was used to determine the relationship between MAOA and WNT5A expression and immune infiltration. The Cancer Genome Atlas (http://www.cancer.gov/ccg/research/genome-sequencing/tcga) open free database was used to download the transcriptomics-related data of PCa and the clinicopathological features and overall survival data of PCa of MAOA, so as to evaluate the effects of MAOA on the disease-free survival of patients with PCa.

Cell–cell communication analysis

The "CellChat" package in R language software was used to infer and analyze intercellular communication. The netVisual circle function was employed to visualize the strength of cell–cell communication networks between CAFs and T cells.

Gene knockdown and overexpression

Short hairpin RNA (sh-RNA) targeting MAOA (sh-MAOA) was purchased from GenePharma Technology (Shanghai, China) for gene knockdown, and sh-RNA was used as the negative control. We transfected the lentivirus according to the method provided by the reagent supplier and screened it with puromycin. The sh-MAOA sequence was 5′-ACGCTGAACCATGAACATTAT-3′. sh-RNA targeting MAOA (sh-MAOA) was purchased from HanBio Technology (Shanghai, China) for gene overexpression. The detailed information on the target vector and the target gene sequence can be found in the online supplemental materials and methods 1. Small interfering RNA (si-RNA) targeting MAOA and scrambled si-RNA as control were also purchased from GenePharma Technology. The MAOA si-RNA target sequences were as follows: 5′-GCUGAACCAUGAACAUUAUTT-3′; 5′-GCAG GTGTAAGTGTGATAATT-3′.

Western blot assays

Western blot analyses were performed using standard protocols.[21] Briefly, cells were lysed in lysis buffer and then subjected to sonication. The lysate was separated by SDS-polyacrylamide gel electrophoresis and transferred onto a polyvinylidene fluoride membrane. Each membrane was first blocked with 5% milk for 2 hours, then incubated with various primary antibodies overnight at 4°C, followed by incubation with secondary antibodies for 2 hours at room temperature, and finally visualized with an enhanced chemiluminescence reagent. Antibodies against the following proteins were used: MAOA (Abcam, ab126751, 1:1000), WNT5A (Proteintech, 29 793–1-AP, 1:700), α-SMA (ServiceBio, GB13044, 1:1000), MYH11 (Santa Cruz, sc-6956, 1:1000), RGS5 (Santa Cruz, sc-514184, 1:1000), β-Actin (Engibody, AT0001, 1:2000).

Immunofluorescence staining

Tissue sections were deparaffinized and subjected to antigen retrieval. Cell permeabilization was performed using 0.1% polyethylene glycol mono-p-isooctylphenyl ether (Triton X-100) (Nacalai Tesque). Tissue was blocked with 2% bovine serum albumin and then stained with the MAOA antibody (Abcam), α-SMA (ServiceBio), WNT5A (Proteintech) CD8 (ServiceBio) NFATC1 (Proteintech) and DAPI (Fujifilm Wako, Osaka, Japan). Results were obtained using a fluorescence microscope (BZ-X810, Keyence, Osaka, Japan).

Immunochemistry

Based on standard protocols,[22] immunochemistry analysis was performed using antibodies against prostate-specific antigen (PSA) (Abcam, ab224799), prostate-specific membrane antigen(PSMA) (Abcam, ab133579).

H&E staining

Fixed hydrated tissue was stained with hematoxylin to color the cell nuclei, and with eosin to color the cytoplasm and other tissue structures. Finally, the sections were embedded in a resin medium to preserve the staining and were observed and analyzed under an optical microscope.

Energy metabolism measurements

Mitochondrial oxygen consumption rates (OCRs) and extracellular acidification rates (ECARs) in cells were measured using an XF Extracellular Flux Analyzer (Seahorse Bioscience, Agilent, Santa Clara, California, USA), according to the manufacturer's instructions.

Flow cytometry and fluorescence-activated cell sorting

PCa xenograft cells were dissociated into single-cell suspensions according to the manufacturer's protocol (Miltenyi Biotec, Germany). The samples were filtered through a 70 µm filter and removed supernatant. Cells were subsequently incubated with fluorescent-conjugated antibodies at 4°C for 30 min. For analysis of the infiltration and exhaustion of $CD8^+$ T cells, single-cell suspensions were stained with Fixable Viability Dye (BioLegend, #423105) at 4°C for 20 min. Cells were subsequently stained with anti-mouse CD45, CD8, and PD-1 and anti-human CD45, CD8, and PD-1 and other antibody panels. Information on the antibodies used for flow cytometry analyses is listed in online supplemental table 1.

Cytoplasmic ROS and calcium concentration detection

For determination of ROS production, WPMY-1/H-PrSC were treated with 10 µM 2',7'-Dichlorodihydrofluorescein (Beyotime) as manufacturer's protocols. The fluorescence intensity of 2',7'-dichlorofluorescein was evaluated by flow cytometry.

Cytoplasmic calcium levels were detected by the Fluo-4 AM probe. In short, after co-culturing with WPMY-1-NC/WPMY-1-sh-MAOA for 48 hours, collect PBMC/JURKAT cells and incubate with 1 mL Fluo-4 AM (2.5 µM) in phosphate-buffered saline (PBS) at 37 °C for 30 min. Thoroughly wash the cell suspension and resuspend in PBS, then analyze by flow cytometry.

Animal experiment

Five to 6 week-old male NOD/ShiLtJGpt-*Prkdc*^{em26Cd52}*Il2rg*^{em26Cd22}/Gpt (NCG) mice, C57BL/6J mice were purchased from GemPharmatech LLC (China). All animals were housed in a barrier environment at the Experimental Animal Center of the Fourth Military Medical University. All experimental animal protocols were approved by the FMMU Institutional Animal Care and Use Committee (Protocol No. 20200417).

Subcutaneously implant bilaterally in NCG mice with PC3 and WPMY-1-NC (left side, 1:3)/PC3 and WPMY-sh-MAOA (right side, 1:3) and unilaterally with a mixture of PC3 and WPMY-1-NC/WPMY-sh-MAOA (1:3) cell lines. One week before the cell line implantation, PBMCs at a concentration of 2×10^7/µL were injected via the tail vein to reconstitute the human immune system. Two weeks after the PBMC implantation, peripheral blood from the mice was collected and the proportion of human CD45$^+$ cells was analyzed by flow cytometry to assess the reconstitution of the human immune system. A proportion of CD45$^+$ cells greater than 25% indicates a successful model construction. After the tumor volume reached approximately 50 mm^3, the unilaterally implanted cell group was treated with α-PD-1 (10 mg/kg, Bio X Cell, # SIM0010) twice a week for three consecutive weeks. The growth of the tumors was dynamically monitored after cell implantation, with tumor volume measured twice a week.

Male C57BL/6J mice aged 5–6 weeks were subcutaneously implanted with a mixed cell line of RM-1 and M-PrSC (1:3). After the tumor volume reached 50 mm^3, the mice were blindly randomly grouped and treated with intraperitoneal injections. The control group received physiological saline, chlorgyline (Clo) group (15 mg/kg, MCE, HY-14197A), phenelzine (Phe) group (20 mg/kg, MCE, HY-B1018A), α-PD-1 (10 mg/kg, Bio X Cell, #BE0146), and the combination group (chlorambucil and α-PD-1). Chlorambucil and Phe were administered three times a week for 2 weeks. α-PD-1 was given once every 3 days for 2 weeks. The growth of the tumors was dynamically monitored after cell implantation, with tumor volume measured twice a week.

Statistical analysis

The data were presented as mean±SE, and were analyzed using GraphPad Prism (GraphPad Software, San Diego, USA). Differences between experimental groups were tested using the Student's t-test and one-way and two-way analysis of variance ($p<0.05$).

RESULTS

Single-cell data reveal the biological functions of stromal MAOA

To deeply understand the role of MAOA in the stromal cells of PCa, we conducted a comprehensive reanalysis of a publicly accessible single-cell transcriptome dataset from PCa (GSE137829). Employing meticulous quality control measures and correction for batch effects, we successfully categorized 25,782 cells into 28 distinct cell subsets (online supplemental figure S1A). By examining the genes specifically expressed within these clusters and using recognized cell marker genes,[23] we identified seven unique cell types (figure 1A, online supplemental figure S1B). Notably, fibroblasts were predominantly found in clusters 3, 7, 22, and 28 (figure 1B). Given the pivotal role of CAFs in tumor progression, we further dissected the fibroblast subpopulations and analyzed their expression profiles. We found that subclusters 2 and 4 exhibited higher transcriptomic similarity to each other, contrasting with subclusters 1 and 3. All subpopulations exhibited the typical characteristics of CAFs, including the elevated expression of specific genes (online supplemental figure S1B). Drawing from previously published gene expression profiles, we classified subclusters 2 and 4 as myofibroblastic cancer-associated fibroblasts with contractile properties (myCAFs, marked by high expression of ACTA2 and RGS5), whereas subclusters 1 and 3 were identified as inflammatory cancer-associated fibroblasts (iCAFs, marked by high expression of PDGFRA and CXCL12) (figure 1C , online supplemental figure S1C). Further analysis revealed that the expression of the MAOA gene was particularly prominent in myCAFs (figure 1D). Western blot results also indicated that the knockout of MAOA can inhibit the expression of myCAFs markers such as MYH11, ACTA2, and RGS5 (online supplemental figure S1D). Moreover, the pseudotime analysis also corroborated that the expression level of MAOA gradually increases with the differentiation of the myCAFs subpopulation, which further implies its significant and indispensable role within the myCAFs subpopulation (online supplemental figure S1E).

To more precisely understand the function of MAOA-positive CAFs within the TME, we designated cluster 4, which exhibits the highest expression of MAOA, as MAOA^{high}CAFs, and cluster 3, with the lowest expression, as MAOA^{low}CAFs (figure 1E). Gene Ontology (GO) enrichment analysis of the differentially expressed genes between these two cell groups indicated that MAOA^{high}CAFs are significantly associated with signaling pathways such as cell junction organization, actin filament-based processes, and nervous system functions; conversely, MAOA^{low}CAFs are linked to pathways including leukocyte differentiation, leukocyte migration, and chemokine activity (figure 1F). Furthermore, CellChat analysis disclosed that, in comparison to MAOA^{high}CAFs, MAOA^{low}CAFs engage in a greater number of ligand-receptor interactions with T cells (online supplemental figure S1F), particularly in their interactions with CD8$^+$ T cells (figure 1G). These insights suggest that MAOA might play a role in modulating the transformation of CAFs and the immune response within stromal cells. In essence, inhibiting MAOA activity in CAFs could potentially induce a phenotypic shift in these cells, thereby enhancing their capacity to promote an immune response.

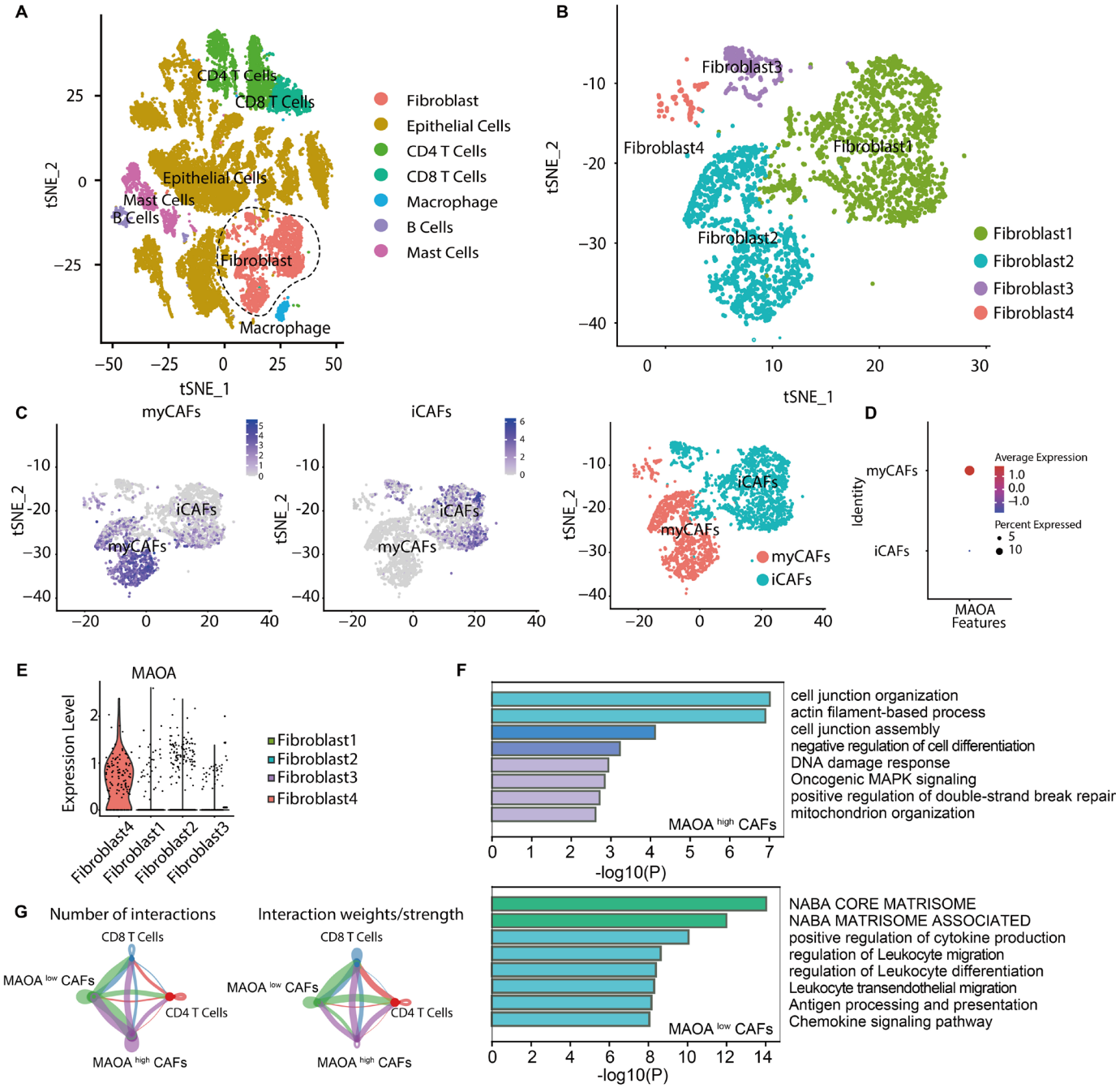

Figure 1 Single-cell data reveal the biological functions of stromal MAOA. (A) The cell type annotation of 25,782 cells using t-distributed stochastic neighbor embedding (t-SNE) and uniform manifold approximation, categorizing them into a total of 7 types, including fibroblast, epithelial cells, CD4$^+$ T cells, CD8$^+$ T cells, macrophage, B cell and mast cells. (B) Through unsupervised clustering and subdivision of the fibroblast population in (A), a t-SNE plot of 4 CAF subclusters was obtained, with the subclusters coded with different colors. (C) t-SNE plots of selected myCAFs markers (ACTA2 and RGS5) and iCAFs markers (PDGFRA and CXCL12), exhibiting specific gene expression signatures in subclusters, two distinct cell subtypes. The intensity of colors indicates the signature scores of myCAFs and iCAFs. (D) The expression of MAOA in iCAFs and myCAFs. (E) The expression levels of MAOA in fibroblast 1, 2, 3, and 4. (F) GO (Gene ontology) functional enrichment on upregulated genes in MAOA^{high}CAFs (upper) and MAOA^{low}CAFs (lower), respectively. The intensity of the color indicates -log10FDR. (G)Cell–cell communication from MAOA^{high}CAFs and MAOA^{low}CAFs to CD8$^+$ T cells and CD4$^+$ T cells. CAFs, cancer-associated fibroblasts; iCAFs, inflammatory cancer-associated fibroblasts; MAOA, monoamine oxidase A; myCAFs, myofibroblastic cancer-associated fibroblasts.

Stromal MAOA is involved in the progression of PCa and is associated with the immunosuppressive microenvironment

To verify the results of single-cell sequencing, we conducted an analysis to compare the expression levels of MAOA in myCAFs and iCAFs. Immunofluorescence (IF) assays revealed that, in contrast to PDGFRA^{high}ACTA2^{low}-CAFs, PDGFRA^{low}ACTA2^{high}CAFs exhibited significantly higher MAOA expression levels (figure 2A). Additionally,

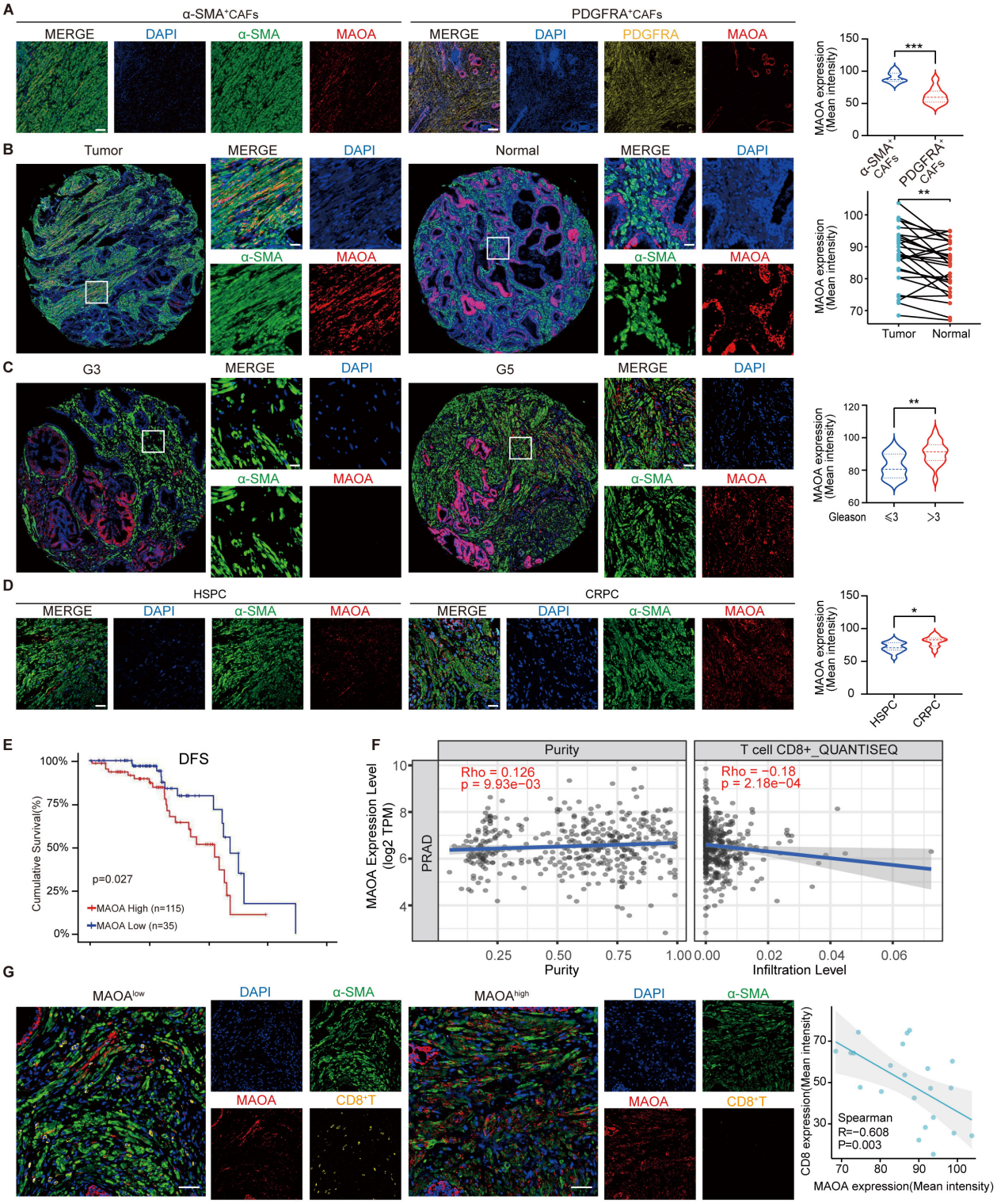

Figure 2 Stromal MAOA is associated with the immunosuppressive microenvironment. (A) Representative images and quantitation of the expression of MAOA in α-SMA$^+$CAFs and PDGFRA$^+$CAFs in prostate cancer. Scale bars, 50 µm. (B) Representative images and quantitation of coimmunostaining of MAOA and α-SMA in normal prostates (n=29) and PCa (n=29). Scale bars, 20 µm. (C) Representative images and quantitation of coimmunostaining of MAOA and α-SMA in PCa progression categorized by low GS (n=53) and high GS (n=65). Scale bars, 20 µm. (D) Representative images and quantitation of MAOA and α-SMA in hormone-sensitive (HSPC, n=20) and castration-resistant (CRPC, n=15) PCa. Scale bars, 50 µm. (E) Kaplan-Meier disease-free survival (DFS, n=150) with either low or high MAOA protein levels. (F) In the TIMER database, increased MAOA expression is negatively correlated with the infiltration of CD8$^+$ T cells. (G) Representative images and quantitation of CD8 in MAOA^{low} and MAOA^{high} of PCa stromal (n=29). Scale bars, 20 µm. CAFs, cancer-associated fibroblasts; DAPI, 4',6-Diamidino-2-Phenylindole; GS,Gleason Score; MAOA, monoamine oxidase A; PCa, prostate cancer; PRAD, Prostate Adenocarcinoma; TIMER, Tumor IMmune Estimation Resource; TPM, Transcripts Per Million.

we noted a reduction in α-SMA expression after MAOA knockdown in WPMY-1 cells (online supplemental figure 2SA). A similar trend was observed after treatment with varying concentrations of MAOA inhibitors (online supplemental figure 2SA). Collectively, these results confirm that MAOA is a pivotal mediator in the transformation of CAFs.

Furthermore, PCa TMA analysis demonstrated that the stromal expression of MAOA in malignant tissue was markedly higher compared with that in normal prostate tissue (figure 2B), and there was a positive correlation between MAOA expression and the Gleason score (figure 2C). IF analysis also showed that MAOA expression increased progressively as PCa advanced from hormone-sensitive PCa to CRPC (figure 2D). Importantly, patients with elevated MAOA expression faced a poorer prognosis (figure 2E). These data collectively affirm the role of stromal MAOA in the progression of PCa and highlight its potential as a therapeutic target for patients with advanced CRPC.

To explore the relationship between stromal MAOA and immunity, we initially used the TIMER database to assess the correlation between MAOA expression and various immune cell populations. Our findings revealed an inverse relationship between MAOA expression and the presence of $CD8^+$ T cells (figure 2F), while a positive association was observed with $FOXP3^+$ T cells, an inverse correlation with M1 macrophages, and a direct correlation with M2 macrophages (online supplemental figure S2B). Given that single-cell sequencing data suggested a more pronounced interaction between CAFs and $CD8^+$ T cells, therefore, we subsequently concentrated our efforts on elucidating the relationship between stromal MAOA and $CD8^+$ T cells. Further analysis of patient TMAs substantiated our hypothesis: there is a negative correlation between the expression levels of stromal MAOA and the extent of $CD8^+$ T cell infiltration (figure 2G).

In vitro inhibition of stromal MAOA better activates the immune killing function of $CD8^+$ T cells

To further explore the intricate interaction between stromal MAOA and $CD8^+$ T cells, we performed in vitro co-culture experiments using established PCa organoids (figure 3A). To minimize the impact of MAOA within the organoids, we selected two organoid lines with relatively low MAOA expression for our experiments (figure 3B). On day 0, WPMY-1 were co-cultured with the organoids. Subsequently, on day 7, PBMCs, which had been preactivated with CD3/CD28 for 1 day, were introduced into the co-culture system (figure 3C). The experimental results indicated that, in comparison to organoids co-cultured with WPMY-1-NC, those co-cultured with WPMY-1-sh-MAOA experienced a further reduction in viability under the influence of PBMCs (figure 3D, online supplemental figure S3A). Additionally, compared with the control group, the co-culture group treated with MAOA inhibitors for 7 days and subsequently stimulated by activated PBMCs showed a further decrease in organoid vitality (figure 3E, online supplemental figure S3B). This finding prompted us to contemplate the potential mechanisms underlying this phenomenon.

To further investigate, we conducted co-culture experiments with WPMY-1 cells and either PBMCs or JURKAT cells, both of which had been preactivated with CD3/CD28 for 1 day, for an additional 24-hour period (figure 3F). The findings indicated a notable elevation in the expression of the activation marker CD69 in both PBMCs and JURKAT cells when co-cultured with WPMY-1-sh-MAOA, as opposed to those co-cultured with WPMY-1-NC (figure 3G). Consistently, there was a significant increase in the proportion of $CD8^+$ T cells expressing IFN-γ and GZMB (figure 3H). However, no such increase in IFN-γ and GZMB expression was observed in JURKAT cells (online supplemental figure S3C), which is presumably attributable to their lineage as $CD4^+$ T cells, a cell type that typically exhibits minimal or no expression of these cytotoxic factors. We also monitored changes in immune exhaustion markers such as PD-1 and CTLA-4, and the results indicate that stromal MAOA does not significantly affect the exhaustion of $CD8^+$ T cells (online supplemental figure S3D). This may be due to the duration and intensity of antigen stimulation, so the exhaustion markers will not change.[24]

Additionally, we cultured PCa cells (C42, DU145, PC3) with the conditioned media derived from WPMY-1-NC and WPMY-1-sh-MAOA for a period of 72 hours (online supplemental figure S3E). Western blot analysis revealed that exposure to conditioned media from WPMY-1-sh-MAOA led to a decrease in PD-L1 expression within the PCa cells and organoids (online supplemental figure S3F). These findings suggest that the inhibition of stromal MAOA in vitro can stimulate the antitumor immune response of $CD8^+$ T cells.

Inhibition of stromal MAOA can suppress the growth of PCa xenografts by activating the immune killing function of $CD8^+$ T cells

To conduct a comprehensive investigation into the role of stromal MAOA, we combined the mouse PCa cell line RM1, which exhibits low MAOA expression, with primary mouse prostate stromal cells (M-PrSC) that display relatively higher MAOA expression (online supplemental figure S4A). This mixture was then subcutaneously inoculated on the abdomen of C57BL/6 mice to establish a xenograft tumor model (figure 4A). Once the subcutaneous tumors reached a volume of 50 mm^3, we administered intraperitoneal injections of the MAOA inhibitors Phe (at a dosage of 20 mg/kg, three times weekly) and Clo (at a dosage of 15 mg/kg, three times weekly), while continuously monitoring the tumor size. The findings demonstrated that the tumor growth rate in the treatment group was significantly reduced compared with the control group (figure 4B, online supplemental figure S4B). Furthermore, the administered drug concentrations did not induce any apparent hepatotoxicity or nephrotoxicity (online supplemental figure S4C). IF analysis

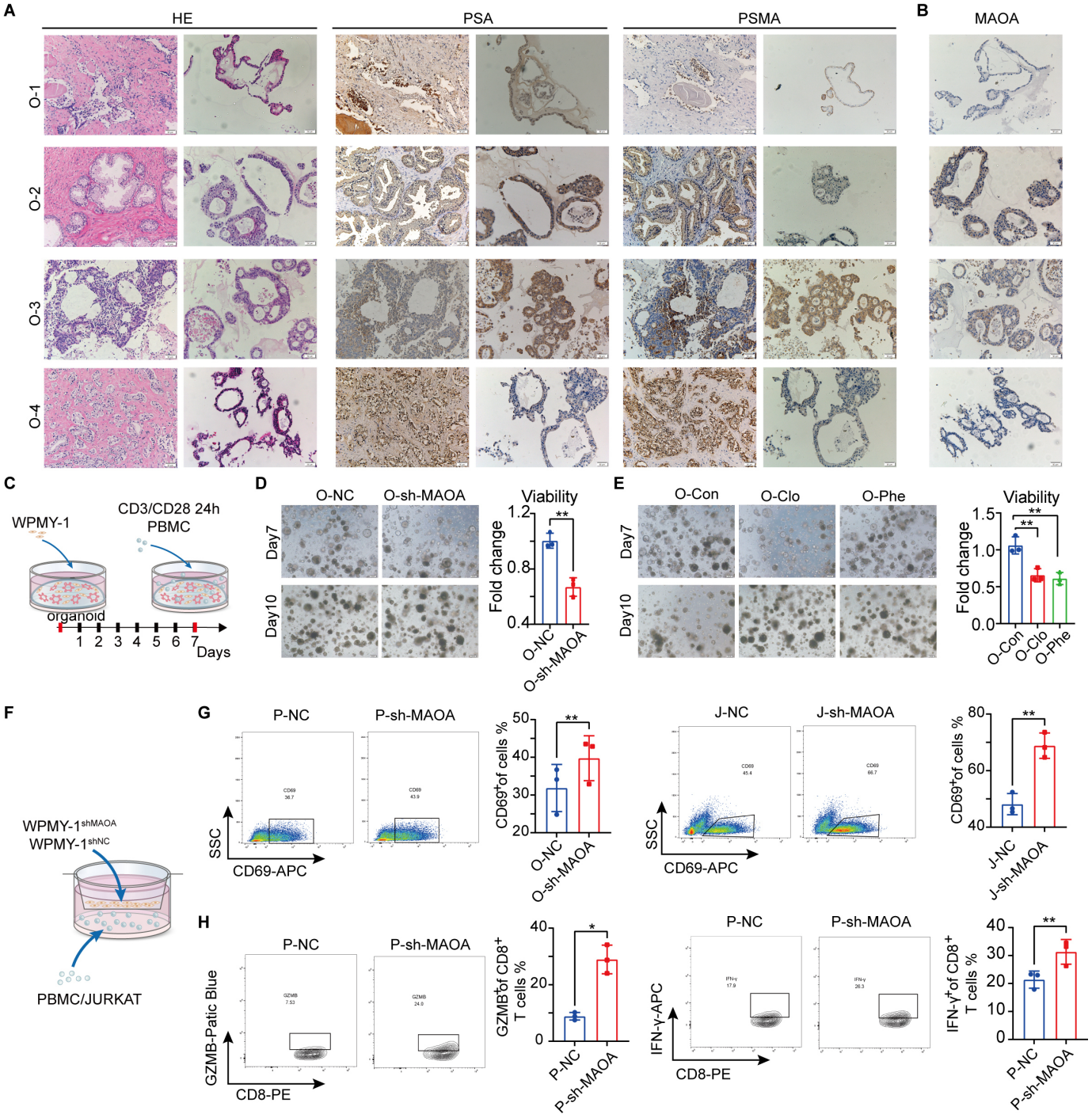

Figure 3 In vitro suppression of stromal MAOA activity significantly enhances the immune response by bolstering the cytotoxic capabilities of $CD8^+$ T cells (A) Histological analysis comparing the tissue structure of organoids with that of native tissue, stained with H&E bars, 50 µm; IHC staining of organoids with antibodies against specific markers of the two germ layers, indicating proper differentiation. Scale bars, 50 µm. (B) Representative images of IHC staining of organoids-expressed MAOA. Scale bars, 50 µm. (C) WPMY-1 and organoid co-culture schematic diagram with PBMC. (D) Representative organoid microscope images using WPMY-1-NC/sh-MAOA. Scale bars, 200 µm. (E) Representative organoid microscope images after treatment with MAOA inhibitors. Scale bars, 200 µm. (F) Schematic diagram of co-culture with WPMY-1-NC/sh-MAOA and PBMC/JURKAT cells. (G) FACS analysis of PBMCs or JURKAT of $CD69^+$ of anti-CD3/CD28-activated after co-culturing WPMY-1-NC or WPMY-1-sh-MAOA (n=3). (H) FACS analysis of $CD8^+$ T cells of $GZMB^+$ and IFN-γ^+ of anti-CD3/CD28-activated after co-culturing WPMY-1-NC or WPMY-1 sh-MAOA (n=3). FACS, fluorescence-activated cell sorting; IHC, immunohistochemistry; MAOA, monoamine oxidase A; PBMC, peripheral blood mononuclear cell; PSA, prostate-specific antigen; PSMA, prostate-specific membrane antigen; sh-MAOA, short hairpin RNA targeting MAOA.

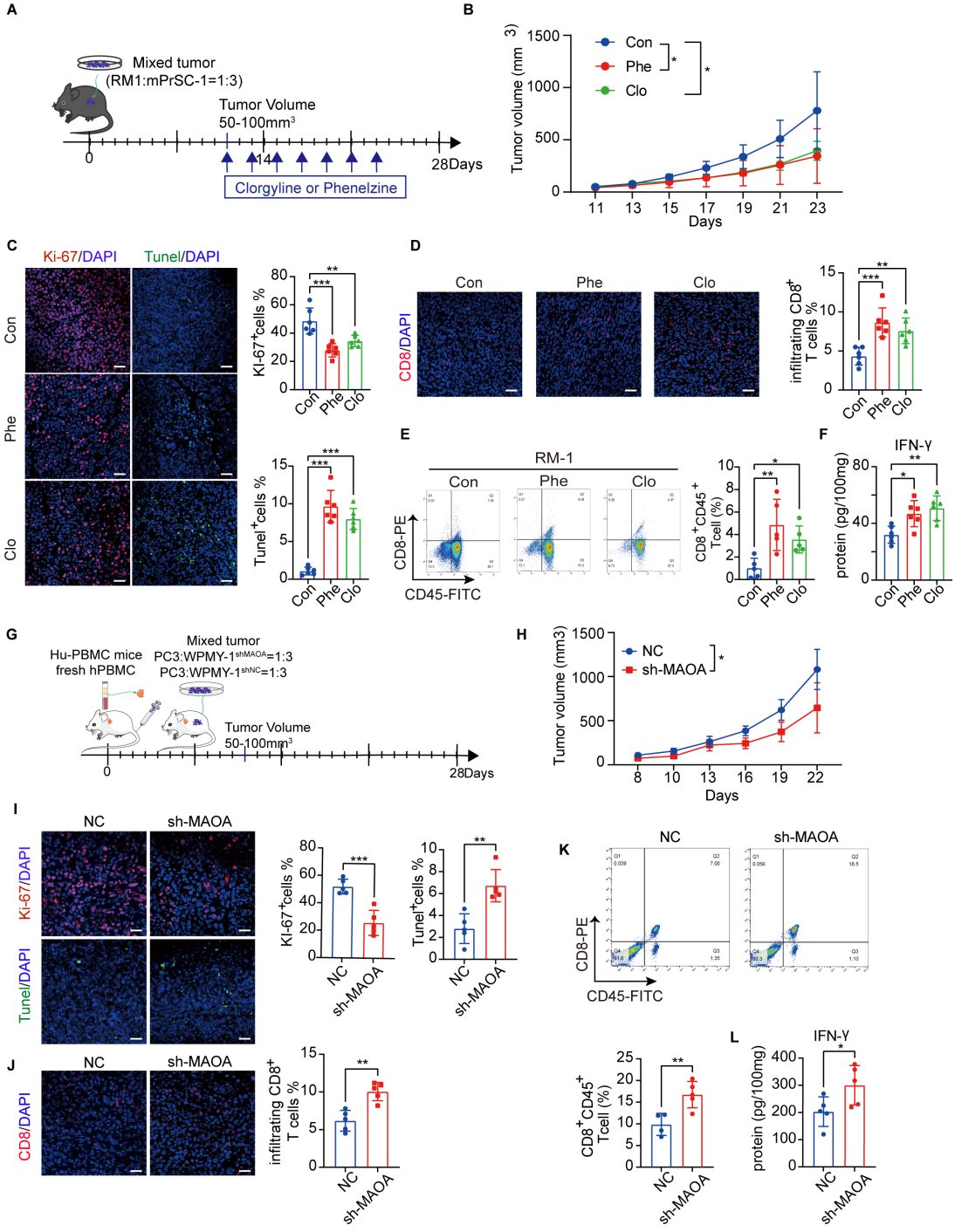

Figure 4 Suppressing stromal MAOA activity in vivo can effectively inhibit the proliferation of prostate cancer xenografts by potentiating the immune-killing function of $CD8^+$ T cells. (A) Schematic diagram of the construction of a subcutaneous tumor graft model in C57BL/6J mice and the drug administration strategy. (B) Tumor growth curves of mice in different treatment groups. (C) Representative images and quantification results of $KI\text{-}67^+$ and $Tunel^+$ in mice from different treatment groups, scale bars, 50 µm. (D) Representative images and quantification results of $CD8^+$ T cells in different treatment groups of mice, scale bars, 50 µm. (E) FACS analysis of the proportion of $CD8^+CD45^+$ T cells in tumor tissues from different treatment groups. (F) ELISA experiments to detect the content of IFN-γ in tumor tissues from different treatment groups. (G) Strategy for the construction of double humanized PCa mouse model and administration. (H) The tumor growth curves of mice in the NC group and the sh-MAOA group. (I) Representative images and quantification results of $KI\text{-}67^+$ and $Tunel^+$ for mice in the NC group and sh-MAOA group, scale bars, 50 µm. (J) Representative images and quantification results of $CD8^+$ T cells in the NC group and sh-MAOA group of mice. Scale bars, 50 µm. (K) FACS analysis of the proportion of $CD8^+CD45^+$ T cells in tumor tissues from NC group and sh-MAOA group. (L) ELISA experiments to detect the content of IFN-γ in tumor tissues from NC group and sh-MAOA group. Clo, chlorgyline; Con, control; DAPI, 4',6-Diamidino-2-Phenylindole; FACS, fluorescence-activated cell sorting; M-PrSC, mouse primary stromal cells; NC, negative control; PBMC, peripheral blood mononuclear cell; PCa, prostate cancer; Phe, phenelzine; sh-MAOA, short hairpin RNA targeting monoamine oxidase A.

revealed that the proportion of KI-67$^+$ cells within the tumors of the treatment group was decreased, while the number of Tunel$^+$ cells increased (figure 4C). Concurrently, there was a significant increase in the number of CD8$^+$ T cells (figure 4D). Flow cytometry analysis also supported this finding, showing a marked increase in the proportion of CD8$^+$CD45$^+$ T cells in the treatment group (figure 4E), along with a substantial rise in the level of IFN-γ within the tumor lysate (figure 4F).

To simulate the human immune system, we developed a double humanized immune-reconstituted mouse model[25] to validate the immune response orchestrated by stromal MAOA; PC3 cells with low MAOA expression (online supplemental figure S4D) alongside WPMY-1-NC/sh-MAOA cells were mixed respectively and subcutaneously transplanted on both the left and right sides of the abdomen of the same H-NCG mouse (figure 4G). As shown in online supplemental figure S4E,F, reconstituted mice were established successfully. Consistent with the results in C57BL/6 mice, the tumor growth rate in reconstituted mice with sh-MAOA mixed tumors was significantly decelerated (figure 4, online supplemental figure S4G). The proportion of KI-67+cells was reduced, while the proportion of Tunel$^+$ cells was elevated(-figure 4I). Additionally, there was a notable increase in the number of CD8$^+$ T cells (figure 4J), and the proportion of CD8$^+$CD45$^+$ T cells was significantly upregulated (figure 4K). Correspondingly, the level of IFN-γ in the tumor lysate was also markedly increased (figure 4L). Collectively, these experimental data confirm that the inhibition of stromal MAOA can activate the cytotoxic function of CD8$^+$ T cells, thereby effectively suppressing the growth of PCa.

Stromal MAOA inhibition boosts WNT5A secretion, enhancing the Ca^{2+}-NFATC1 pathway in CD8$^+$ T cells to suppress PCa xenograft growth

In order to explore the molecular mechanisms through which stromal MAOA contributes to tumor immune suppression, we employed RNA sequencing technology (RNA-Seq) to conduct a comparative analysis of gene expression profiles between the WPMY-1-NC and sh-MAOA cell lines. Our findings revealed that within the genes exhibiting an enrichment fold greater than 1, there were 2,596 upregulated and 4,470 downregulated genes in the sh-MAOA group (online supplemental figure S5A). GO enrichment analysis indicated that immune-related pathways, including lymphocyte migration, T cell migration, and chemokine signaling, were significantly enriched in the sh-MAOA group (figure 5A). Notably, the enrichment of the secretory protein WNT5A was particularly prominent among these immune-related pathways (figure 5B). Previous studies have suggested that WNT5A can facilitate antigen processing and presentation, activate immune responses,[26] and inhibit bone metastasis of PCa,[27] but its specific role in PCa immunotherapy remains to be clarified. Based on these insights, we hypothesize that the inhibition of stromal MAOA may enhance the secretion of WNT5A, thereby stimulating the antitumor immune response of CD8$^+$ T cells.

On ablating MAOA in stromal cells and clinical patient samples, we observed an increase in WNT5A expression levels (online supplemental figure S5B,C), aligning with the RNA-seq data and suggesting that WNT5A serves as a pivotal downstream effector molecule of MAOA. Furthermore, we administered the WNT5A mimetic peptide FOXY5 (at a dosage of 2 mg/kg, four times weekly) to C57BL/6 mice and noted a significant suppression of RM-1 mixed tumor growth (figure 5C). This was accompanied by an elevation in the proportion of CD8$^+$CD45$^+$ T cells and a reduction in the proportion of PD-1$^+$ cells (figure 5D). Moreover, the results of bioinformatics analysis also confirm that the expression of WNT5A is inversely proportional to CD8$^+$ T cells (online supplemental figure S5D). These findings support the hypothesis that WNT5A activates the immune response of CD8$^+$ T cells, thereby impeding the growth of PCa.

Given that the WNT5A/Ca^{2+} signaling pathway is a non-canonical WNT signaling pathway[28] and considering the Ca^{2+}-NFATC1 signaling pathway's intimate association with the activation and effector functions of CD8$^+$ T cells,[29–31] we proceeded to investigate the potential involvement of this pathway following the inhibition of stromal MAOA. Using flow cytometry to monitor intracellular Ca^{2+} flux, we discovered a notable increase in Ca^{2+} levels in both PBMCs and JURKAT cells after co-culture with WPMY-1-sh-MAOA cells (figure 5E). IF analysis further revealed that, post anti-CD3/CD28 activation, there was enhanced nuclear translocation of NFATC1 in CD8$^+$ T cells and JURKAT cells co-cultured with WPMY-1-sh-MAOA cells (figure 5F). Subsequent treatment with the WNT5A/Ca^{2+} signaling pathway inhibitor BOX5 (100 μM) led to a significant reduction in the expression ratio of CD69 in PBMCs and JURKAT cells (figure 5G), and the proportion of IFN-γ and GZMB positive cells in CD8$^+$ T cells also decreased (figure 5H). Collectively, these results underscore the WNT5A/Ca^{2+}-NFATC1 signaling pathway as a critical mediator of the CD8$^+$ T cell immune response regulated by MAOA.

In summary, the inhibition of stromal MAOA not only enhances the production of the WNT5A secretory protein but also activates the cytotoxic effect of CD8$^+$ T cells via the Ca^{2+}-NFATC1 signaling pathway, thereby conferring antitumor effects. This novel finding offers a new perspective and a potential therapeutic strategy for the immunotherapy of PCa.

Stromal MAOA regulates the production of WNT5A by modulating mitochondrial function

After establishing the regulatory relationship between stromal MAOA and WNT5A, we further explored the underlying molecular mechanisms. Given that previous studies have highlighted the critical role of oxidative stress in promoting the formation of a reactive stroma in PCa,[32 33] furthermore ROS in the TME can adversely affect immune function. We hypothesized that MAOA might

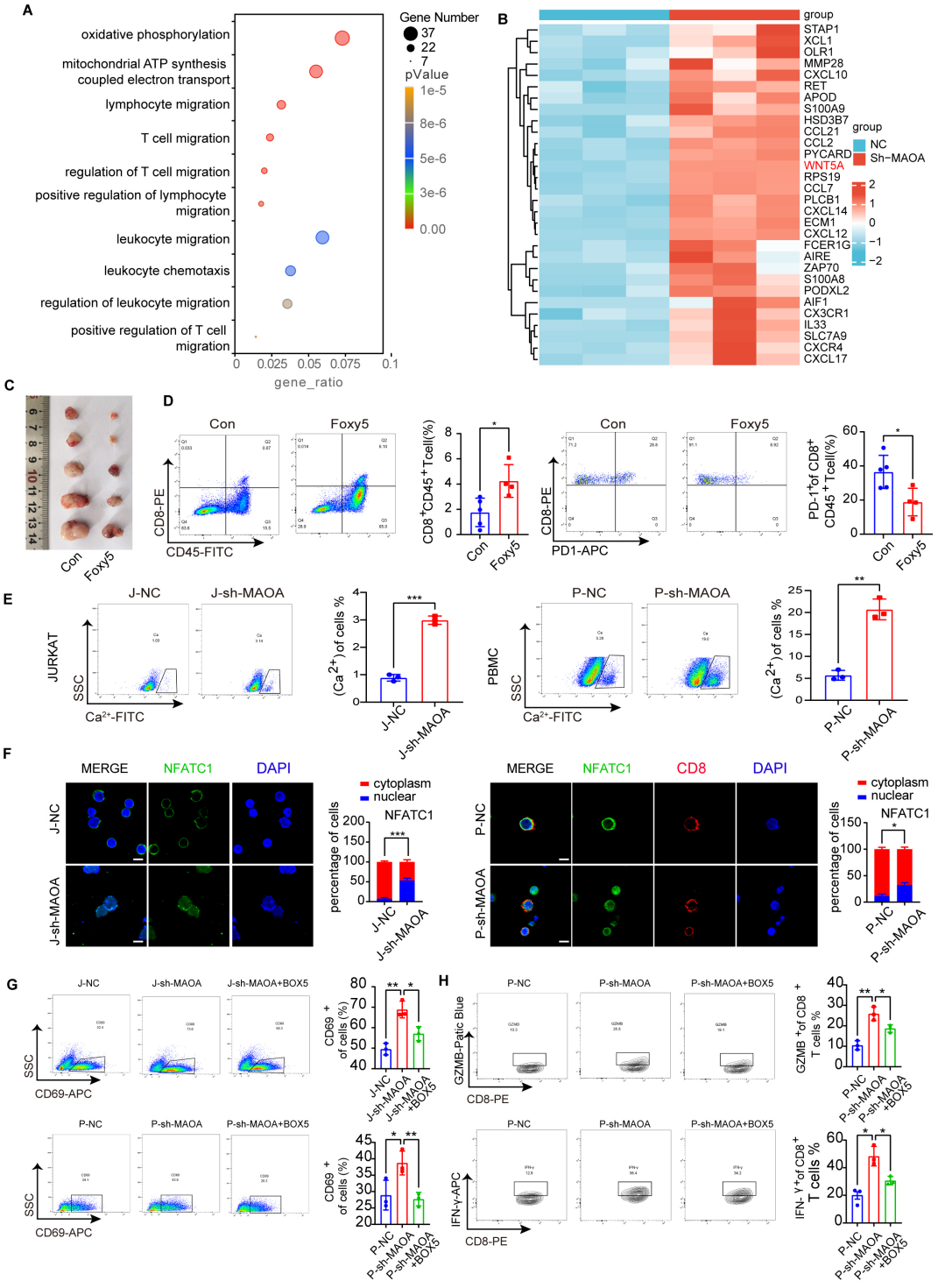

Figure 5 Inhibition of stromal MAOA can suppress the growth of prostate cancer xenografts by enhancing the secretion of WNT5A, which in turn activates the Ca^{2+}-NFATC1 signaling pathway within $CD8^+$ T cells. (A) GO enrichment analysis of differential genes between the WPMY-1-NC and sh-MAOA groups. (B) Heatmap showing the enrichment levels of differential genes between WPMY-1-NC and sh-MAOA groups. (C) Actual photos of tumor sizes in control and FOXY5 treatment groups of C57BL/6J mice. (D) FACS analysis monitoring of the proportion and quantification results of $CD8^+CD45^+$ and $CD8^+CD45^+PD\text{-}1^+$ in tumor tissues of mice in the control and FOXY5 treatment groups. (E) FACS analysis detection of the intracellular Ca^{2+} flux in JURKAT and PBMC cells after co-culture of WPM-1-NC and sh-MAOA. (F) Representative images and quantification results of NFATC1 nuclear translocation in JURKAT and PBMC cells after co-culture of WPM-1 NC and sh-MAOA. Scale bars, 10 µm. (G) FACS analysis detection of the proportion and quantification results of $CD69^+$ in JURKAT and PBMC cells among different treatment groups. (H) FACS analysis detection of the content and quantification results of IFN-γ and GZMB in JURKAT and PBMC cells in different treatment groups. DAPI, 4',6-Diamidino-2-Phenylindole; FACS, fluorescence-activated cell sorting; FITC, Fluorescein Isothiocyanate; GO, Gene Ontology; MAOA, monoamine oxidase A; NC, negative control; PBMC, peripheral blood mononuclear cell; sh-MAOA, short hairpin RNA targeting MAOA; SSC, Side Scatter.

contribute to the production of ROS through its enzymatic oxidase activity, thereby influencing the expression of WNT5A secretory proteins. To test this hypothesis, we employed flow cytometry and discovered that, in comparison to the control group, the levels of endogenous ROS in WPMY-1 and H-PrSC cells with MAOA knockdown were notably diminished (figure 6A). Furthermore, overexpression of MAOA increased the levels of ROS production in WPMY-1 cells (online supplemental figure S6). Gene set enrichment analysis corroborated these findings, revealing that in WPMY-1 cells with silenced MAOA, the "negative regulation of response to oxidative stress" pathway was significantly enriched (figure 6B). To verify whether ROS is a critical mediator in the regulation of WNT5A by stromal MAOA, we treated WPMY-1-NC cells with the ROS scavenger NAC, which led to an increase in WNT5A protein expression. Conversely, the introduction of exogenous H_2O_2 decreased the WNT5A protein level in WPMY-1sh-MAOA cells, with H-PrSC cells exhibiting analogous responses (figure 6C). These results substantiate that MAOA may modulate the expression of WNT5A via ROS.

Additionally, we investigated the mechanism of how MAOA affects the production of ROS. Research has indicated that ROS generation at mitochondrial sites can disrupt the electron transport chain, thereby inhibiting mitochondrial oxidative phosphorylation. This inhibition of oxidative phosphorylation reduces oxygen consumption, which in turn promotes ROS generation. Thus, we hypothesize that MAOA may stimulate the production of ROS by driving this vicious cycle.[34 35] Using Seahorse XF technology, we observed a marked decrease in both the OCR and ECAR in WPMY-1 sh-MAOA cells compared with the control group (figure 6D), although there was no significant difference in the overall rate of ATP production, WPMY-1 sh-MAOA cells exhibited a tendency to produce ATP through oxidative phosphorylation (figure 6E).

In a subsequent experiment, we co-cultured untreated and NAC-treated cells with PBMCs and JURKAT cells for 48 hours. Flow cytometry revealed that in the NAC-treated group, the expression ratio of CD69 in PBMCs and JURKAT cells was significantly enhanced (figure 6F). Concurrently, the proportion of IFN-γ and GZMB positive cells within $CD8^+$ T cells also increased (figure 6G). These findings suggest that MAOA modulates the production of WNT5A by regulating ROS levels, thereby significantly influencing the activation and functionality of $CD8^+$ T cells.

Inhibition of stromal MAOA sensitizes PCa cells to ICIs

Our findings demonstrate that the suppression of stromal MAOA expression can markedly enhance T-cell infiltration across various PCa models. Consequently, we hypothesize that inhibiting MAOA activity could potentially augment the responsiveness of PCa to ICIs. As shown in figure 7A, we established mixed tumors in male C57BL/6 mice and administered treatments with Clo or anti-PD-1 antibody. The data (figure 7B) indicated that, as anticipated, Clo treatment decelerated tumor growth, while anti-PD-1 therapy further suppressed the growth of RM-1 allografts on the basis of Clo treatment. Moreover, the tumor growth reduction in C57BL/6 mice coincided with elevated WNT5A expression, heightened $CD8^+$ T-cell infiltration, and increased levels of IFN-γ in tumor lysates (figure 7C). In the immune-reconstructed mouse model, we also observed similar phenomena (figure 7D–7F). Collectively, these results imply that the inhibition of stromal MAOA activity may enhance the additional tumor-suppressive effect of anti-PD-1 treatment.

In conclusion, our study emphasizes the role of stromal MAOA in modulating the immune microenvironment of PCa. The inhibition of stromal MAOA has been shown to enhance the immune infiltration of $CD8^+$ T cells within PCa. Mechanistically, this inhibition may decrease mitochondrial ROS production, which in turn upregulates WNT5A expression and activates the cytotoxic function of $CD8^+$ T cells through the modulation of the Ca^{2+}-NFATC1 signaling pathway (figure 7G). These insights not only clarify the regulatory mechanisms by which stromal MAOA influences the immunosuppressive microenvironment of PCa but also lay a theoretical foundation for the clinical application of MAOA inhibitors in combination with ICIs for the treatment of PCa.

DISCUSSION

Recent studies including ours demonstrated the prominent role of tumor MAOA in regulating PCa development and metastasis.[17 36] MAOIs have shown positive results in phase II clinical trials for the treatment of recurrent PCa, exhibiting a significant decrease in PSA levels,[37] providing strong evidence for the potential strategy of using MAOIs in the treatment of PCa. Most importantly, MAOA-mediated reprogramming of stromal fibroblasts promotes prostate tumorigenesis and cancer stemness, providing a rationale for targeting stromal MAOA to treat PCa. However, the functional and mechanistic roles of MAOA in PCa stromal cells during PCa immunotherapy remain completely unknown.

Stromal cells such as CAFs are essential components of the tumor immune microenvironment (TIME) and represent promising targets to enhance the immunotherapy response.[38–41] However, therapeutic strategies targeting CAFs are not potent.[42] Emerging evidence indicates that the interaction between CAFs and immune cells plays a crucial role in the development of PCa. Some CAF subtypes contribute to enhancing the immunosuppressive environment of PCa, implying that targeting CAFs to augment tumor responsiveness to immunotherapy by modulating the phenotype and function of CAFs.

Therefore, in this study, we emphasize the important role of MAOA in the CAFs of PCa and reveal its potential as an immunotherapy sensitizer. MAOA inhibition changes the phenotype of CAFs, thereby altering their secretome and affecting the immune status of the TIME.

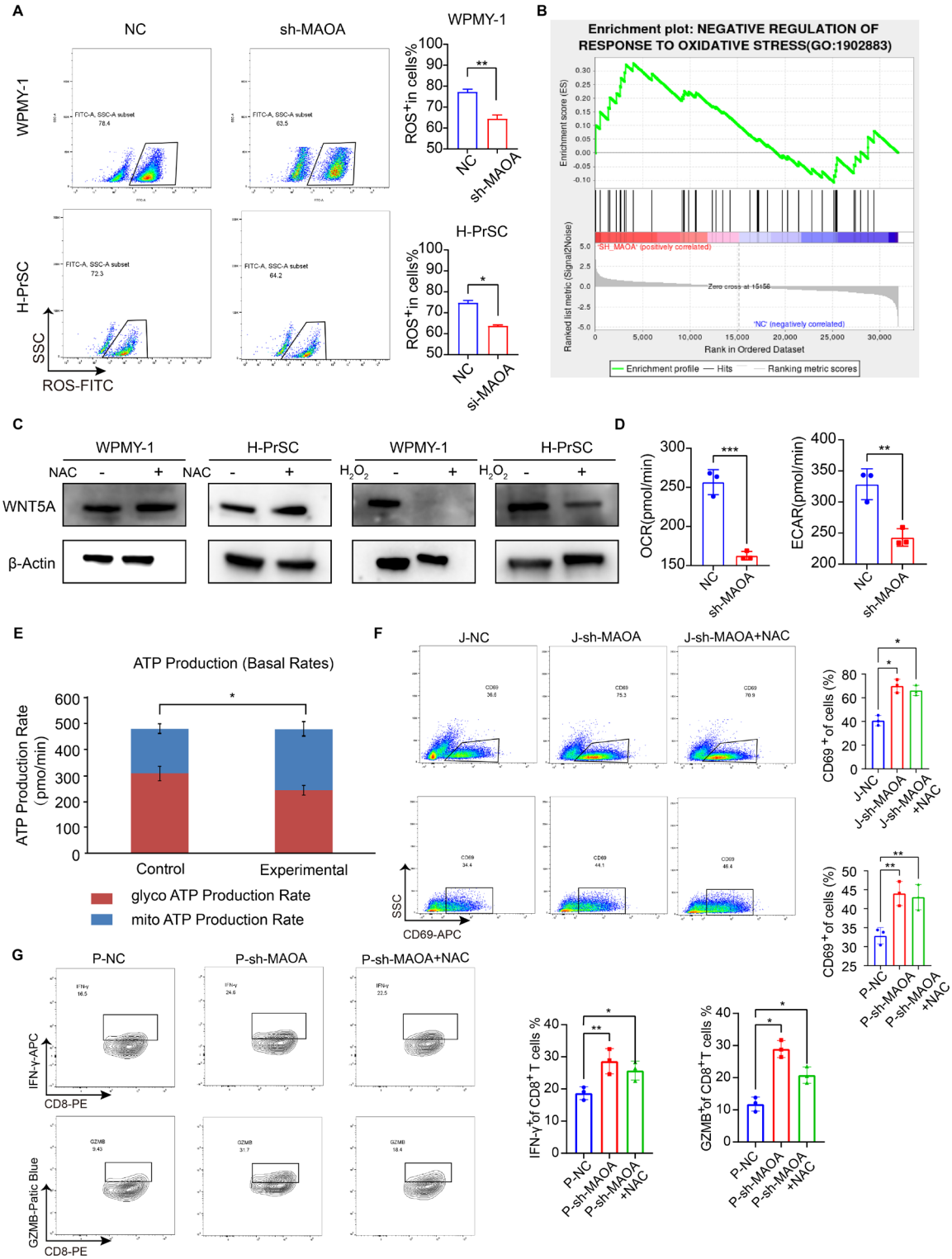

Figure 6 Stromal MAOA regulates the production of WNT5A by modulating mitochondrial function. (A) Determination of ROS content in WPMY-1 and H-PrSC cells in the NC group and the sh-MAOA group. (B) Results of gene enrichment analysis (GSEA) for the WPMY-1 NC group and the sh-MAOA group. (C) Changes in the protein expression levels of WNT5A after WPMY-1 and H-PrSC cells are treated with NAC and H_2O_2. (D) Seahorse XF experiments were used to measure the oxygen consumption rate (OCR) and extracellular acidification rate (ECAR) in the WPMY-1 NC and sh-MAOA groups. (E) ATP production rate in WPMY-1 NC and sh-MAOA cells. (F) The proportion of $CD69^+$ in JURKAT and PBMC cells after co-culturing with WPMY-1 cells treated and untreated with NAC. (G) The proportion of IFN-γ and GZMB in $CD8^+$ T cells after co-culturing PBMC with WPMY-1 cells treated and untreated with NAC. ATP, Adenosine Triphosphate; FITC, Fluorescein Isothiocyanate; H_2O_2, hydrogen peroxide; H-PrSC, human primary prostate cancer stromal cells; MAOA, monoamine oxidase A; NAC, N-acetylcysteine; PBMC, peripheral blood mononuclear cell; ROS, Reactive Oxygen Species; sh-MAOA, short hairpin RNA targeting MAOA; si-MAOA, small interfering RNA targeting MAOA; SSC, Side Scatter Side Scatter .

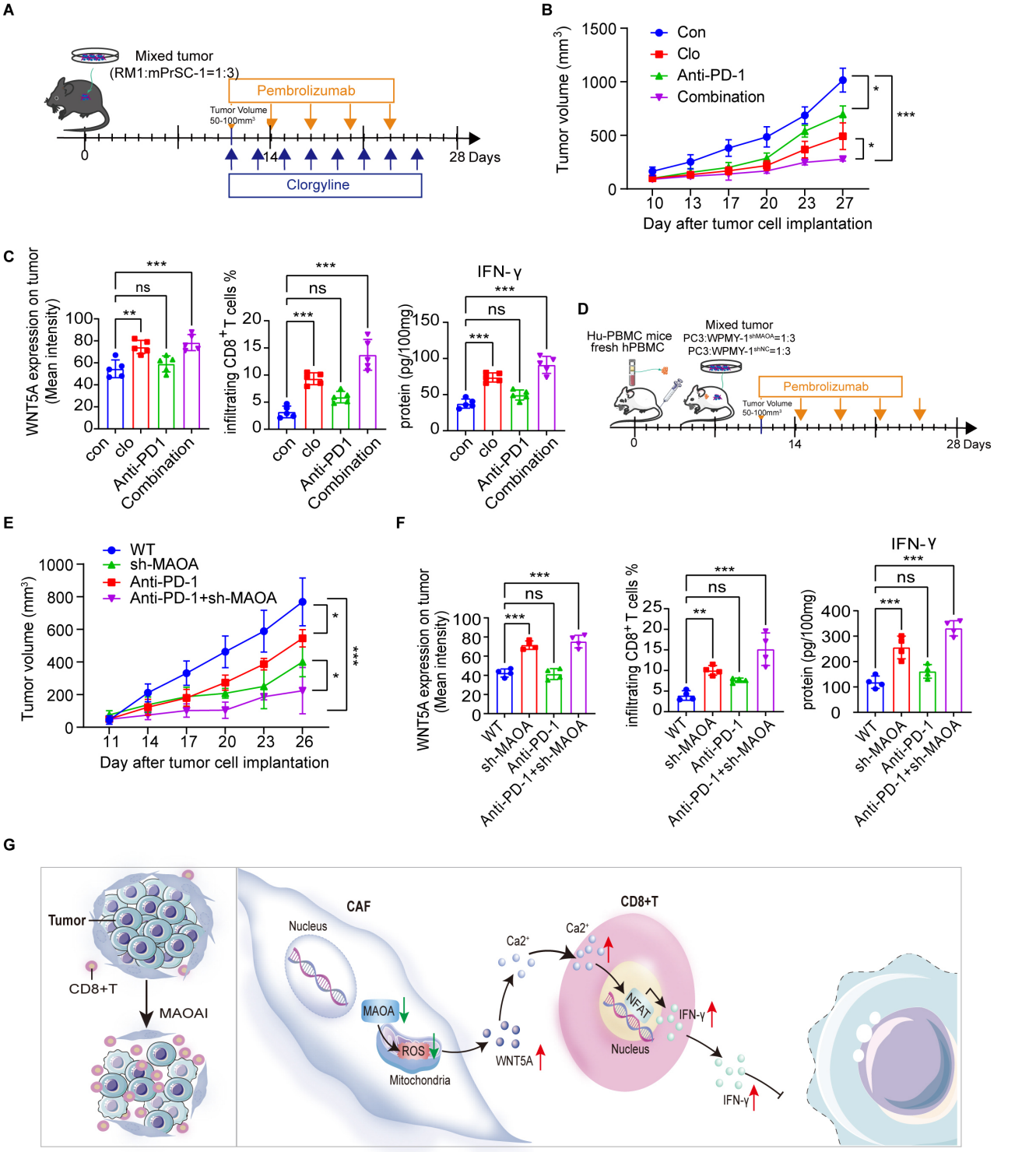

Figure 7 Inhibition of stromal MAOA sensitizes prostate cancer cells to the therapeutic effects of immune checkpoint inhibitors. (A) Strategy for the construction of subcutaneous tumor xenograft model in C57BL/6J mouse model and administration. (B) Tumor growth curves of mice in different treatment groups. (C) The expression of WNT5A, the proportion of $CD8^+$ T cells, and the content of IFN-γ in different treatment groups of mice tumor tissues. (D) Strategy for the construction of double humanized PCa mouse model and administration. (E) Tumor growth curves of mice in different treatment groups. (F) The expression of WNT5A, the proportion of $CD8^+$ T cells, and the content of IFN-γ in different treatment groups of mice tumor tissues. (G) A schematic diagram of the mechanism by which inhibiting MAOA in tumor-associated fibroblasts exerts antitumor effects. Availability of data and material**:** the datasets generated during and/or analyzed during the current study are available from the corresponding author on reasonable request. CAF, cancer-associated fibroblast; Clo, chlorgyline; Con, Control; MAOA, monoamine oxidase A; M-PrSC, mouse primary stromal cells; ns, not significant; PBMC, peripheral blood mononuclear cell; PCa, prostate cancer; PD-1, programmed cell death protein-1; ROS, Reactive Oxygen Species; sh-MAOA, short hairpin RNA targeting MAOA; WT, Wild Type.

The results of single-cell sequencing show MAOA's specific biological functions in CAF subtypes. Such as the development of myCAFs is closely linked to MAOA levels and CAFs exhibiting reduced MAOA expression are significantly correlated with leukocyte migration, differentiation, and chemokine production. This implies that MAOA expression levels could potentially influence the TIME. Further analysis using TMAs has revealed that stromal MAOA is involved in the advancement of PCa, with higher MAOA expression levels being associated with a poorer prognosis.

Our co-culture experiments demonstrated that inhibition of stromal MAOA significantly suppresses the proliferation of PCa organoids by activating the immune response of $CD8^+$ T cells, and this inhibition makes PCa cells sensitive to ICIs, enhancing the infiltration capacity and functionality of $CD8^+$ T cells in suppressing the growth of xenograft tumors. Furthermore, we also examined the impact of changes in MAOA expression on immune exhaustion markers PD-1 and CTLA-4. The results indicated that changes in MAOA expression may not significantly affect the expression levels of these exhaustion markers. This suggests that we need to further search for more specific exhaustion markers to accurately measure the impact of MAOA on immune suppression. In summary, our research has strongly confirmed the therapeutic potential of MAOA as a target. Combining MAOA inhibition and ICIs displays the potential synergistic therapeutic effects. Thus, it offers a rationale for the development of novel combination treatment strategies.

Previous studies have fully reported that MAOA is primarily mediated by excess ROS production to affect the behavior of tumor cells. However, the regulatory mechanism by which MAOA affects the production of ROS is not yet clear. Our study reveals that MAOA can affect the generation of mitochondrial ROS by regulating the respiratory function of mitochondria, including a significant increase in OCR and ECAR. Consequently, disrupting mitochondrial oxidative phosphorylation and enhancing the specific signaling pathways by which stromal MAOA influences mitochondrial function require further elucidation.

WNT5A, an atypical WNT signaling molecule, plays a pivotal role in cancer progression, due to its abnormal activation or inhibition of signal transduction pathways.[43–45] While WNT5A has been identified to inhibit bone metastasis in PCa, its precise role within the immune microenvironment warrants further investigation. Our research, employing RNA sequencing analysis post-MAOA knockout, uncovered extensive alterations in gene expression profiles, especially in immune-related pathways. Notably, the enrichment of WNT5A was the most pronounced among these changes. MAOA can regulate the production of WNT5A through modulation of ROS levels, which in turn influences the activation of $CD8^+$ T cells. The inhibition of stromal MAOA suppresses the growth of PCa xenografts by promoting the secretion of WNT5A, leading to the activation of the Ca^{2+}-NFATC1 signaling pathway in $CD8^+$ T cells. These insights into the regulatory mechanism of MAOA on WNT5A secretion in the stroma offer a novel perspective on the role of MAOA within TIME.

Additionally, this study still has its shortcomings. The primary fibroblasts and organoids isolated may not be sufficiently representative or comprehensive, thus failing to encompass the full spectrum of conditions encountered in all clinical patients. Consequently, in future studies, it will be necessary to increase the sample size and conduct further validation efforts. This will enable us to more precisely ascertain the viability and efficacy of MAOA as a therapeutic target. In summary, our findings highlight the multifaceted roles of stromal MAOA in PCa progression and demonstrate its potential as a therapeutic target. Inhibition of stromal MAOA could offer a novel immunotherapeutic approach for patients with PCa, especially for those who are resistant to traditional treatment and have high levels of stromal MAOA expression.

Acknowledgements We thank ServiceBio (Wuhan, China) for technical support. We thank Ms Caiqin Zhang, Mr Yong Zhao, Ms Hanmu Chen, Mr Pengpeng Wu and Ms Chenyang Zhang (Laboratory Animal Center) for assistance with the animal study.

Contributors ZZ: Investigation, Data curation, Methodology, writing—original draft. YH: Investigation, formal analysis, writing—original draft. HL: Data curation, resources. TL: Formal analysis. XH: Data curation, formal analysis. YM: Investigation. MH: Resources. ML: Investigation. LY: Conceptualization, writing—review and editing. CS: Funding acquisition, project administration, writing—review and editing. CS is the guarantor.

Funding The work was supported by the National Natural Science Foundation of China (32270566 and 32070532) and Shaanxi Province Innovation Capability Support Plan (2022PT-38).

Competing interests No, there are no competing interests.

Patient consent for publication Not applicable.

Ethics approval This study involves human participants and was approved by Xijing Hospital Clinical Research Ethics Committee (No. KY20173028-1). Participants gave informed consent to participate in the study before taking part.

Provenance and peer review Not commissioned; externally peer reviewed.

Data availability statement Data are available upon reasonable request. All data relevant to the study are included in the article or uploaded as supplementary information. The datasets generated during and/or analysed during the current study are available from the corresponding author on reasonable request.

ORCID iDs
Tong Lu http://orcid.org/0000-0001-5691-9209
Changhong Shi http://orcid.org/0000-0001-7490-3593

REFERENCES

1 Sung H, Ferlay J, Siegel RL, *et al*. Global Cancer Statistics 2020: GLOBOCAN Estimates of Incidence and Mortality Worldwide for 36 Cancers in 185 Countries. *CA Cancer J Clin* 2021;71:209–49.
2 Rebello RJ, Oing C, Knudsen KE, *et al*. Prostate cancer. *Nat Rev Dis Primers* 2021;7:9.
3 Morgan RA, Dudley ME, Wunderlich JR, *et al*. Cancer Regression in Patients After Transfer of Genetically Engineered Lymphocytes. *Science* 2006;314:126–9.
4 Hodi FS, O'Day SJ, McDermott DF, *et al*. Improved survival with ipilimumab in patients with metastatic melanoma. *N Engl J Med* 2010;363:711–23.
5 Brahmer JR, Tykodi SS, Chow LQM, *et al*. Safety and activity of anti-PD-L1 antibody in patients with advanced cancer. *N Engl J Med* 2012;366:2455–65.
6 Beer TM, Kwon ED, Drake CG, *et al*. Randomized, Double-Blind, Phase III Trial of Ipilimumab Versus Placebo in Asymptomatic or Minimally Symptomatic Patients With Metastatic Chemotherapy-Naive Castration-Resistant Prostate Cancer. *JCO* 2017;35:40–7.
7 Topalian SL, Hodi FS, Brahmer JR, *et al*. Safety, activity, and immune correlates of anti-PD-1 antibody in cancer. *N Engl J Med* 2012;366:2443–54.
8 Petrylak DP, Loriot Y, Shaffer DR, *et al*. Safety and Clinical Activity of Atezolizumab in Patients with Metastatic Castration-Resistant Prostate Cancer: A Phase I Study. *Clin Cancer Res* 2021;27:3360–9.
9 Fiori ME, Di Franco S, Villanova L, *et al*. Cancer-associated fibroblasts as abettors of tumor progression at the crossroads of EMT and therapy resistance. *Mol Cancer* 2019;18:70.
10 Joshi RS, Kanugula SS, Sudhir S, *et al*. The Role of Cancer-Associated Fibroblasts in Tumor Progression. *Cancers (Basel)* 2021;13:1399.
11 Kobayashi H, Enomoto A, Woods SL, *et al*. Cancer-associated fibroblasts in gastrointestinal cancer. *Nat Rev Gastroenterol Hepatol* 2019;16:282–95.
12 Farhood B, Najafi M, Mortezaee K. Cancer-associated fibroblasts: Secretions, interactions, and therapy. *J Cell Biochem* 2019;120:2791–800.
13 Lakins MA, Ghorani E, Munir H, *et al*. Cancer-associated fibroblasts induce antigen-specific deletion of CD8 $^{+}$ T Cells to protect tumour cells. *Nat Commun* 2018;9:948.
14 Mao X, Xu J, Wang W, *et al*. Crosstalk between cancer-associated fibroblasts and immune cells in the tumor microenvironment: new findings and future perspectives. *Mol Cancer* 2021;20:131.
15 Shih JC, Chen K, Ridd MJ. Monoamine oxidase: from genes to behavior. *Annu Rev Neurosci* 1999;22:197–217.
16 Li J, Pu T, Yin L, *et al*. MAOA-mediated reprogramming of stromal fibroblasts promotes prostate tumorigenesis and cancer stemness. *Oncogene* 2020;39:3305–21.
17 Wu JB, Yin L, Shi C, *et al*. MAOA-Dependent Activation of Shh-IL6-RANKL Signaling Network Promotes Prostate Cancer Metastasis by Engaging Tumor-Stromal Cell Interactions. *Cancer Cell* 2017;31:368–82.
18 Wei J, Yin L, Li J, *et al*. Bidirectional Cross-talk between MAOA and AR Promotes Hormone-Dependent and Castration-Resistant Prostate Cancer. *Cancer Res* 2021;81:4275–89.
19 Yin L, Li J, Wang J, *et al*. MAOA promotes prostate cancer cell perineural invasion through SEMA3C/PlexinA2/NRP1-cMET signaling. *Oncogene* 2021;40:1362–74.
20 Wang X, Li B, Kim YJ, *et al*. Targeting monoamine oxidase A for T cell-based cancer immunotherapy. *Sci Immunol* 2021;6:eabh2383.
21 Sule R, Rivera G, Gomes AV. Western blotting (immunoblotting): history, theory, uses, protocol and problems. *Biotechniques* 2023;75:99–114.
22 Klümper N, Ralser DJ, Ellinger J, *et al*. Membranous NECTIN-4 Expression Frequently Decreases during Metastatic Spread of Urothelial Carcinoma and Is Associated with Enfortumab Vedotin Resistance. *Clin Cancer Res* 2023;29:1496–505.
23 Zhang Y, Fan A, Li Y, *et al*. Single-cell RNA sequencing reveals that HSD17B2 in cancer-associated fibroblasts promotes the development and progression of castration-resistant prostate cancer. *Cancer Lett* 2023;566:216244.
24 Franco F, Jaccard A, Romero P, *et al*. Metabolic and epigenetic regulation of T-cell exhaustion. *Nat Metab* 2020;2:1001–12.
25 Guo W, Qiao T, Li H, *et al*. Peripheral CD8+PD-1+ T cells as novel biomarker for neoadjuvant chemoimmunotherapy in humanized mice of non-small cell lung cancer. *Cancer Lett* 2024;597:217073.
26 Sarraf TR, Sen M. Wnt5A signaling supports antigen processing and CD8 T cell activation. *Front Immunol* 2022;13:960060.
27 Ren D, Dai Y, Yang Q, *et al*. Wnt5a induces and maintains prostate cancer cells dormancy in bone. *J Exp Med* 2019;216:428–49.
28 Zhan T, Rindtorff N, Boutros M. Wnt signaling in cancer. *Oncogene* 2017;36:1461–73.
29 Cong J, Liu P, Han Z, *et al*. Bile acids modified by the intestinal microbiota promote colorectal cancer growth by suppressing CD8^{+} T cell effector functions. *Immunity* 2024;57:876–89.
30 Klein-Hessling S, Muhammad K, Klein M, *et al*. NFATc1 controls the cytotoxicity of CD8+ T cells. *Nat Commun* 2017;8:511.
31 Macian F. NFAT proteins: key regulators of T-cell development and function. *Nat Rev Immunol* 2005;5:472–84.
32 Valencia T, Kim JY, Abu-Baker S, *et al*. Metabolic reprogramming of stromal fibroblasts through p62-mTORC1 signaling promotes inflammation and tumorigenesis. *Cancer Cell* 2014;26:121–35.
33 Martinez-Outschoorn UE, Balliet RM, Rivadeneira DB, *et al*. Oxidative stress in cancer associated fibroblasts drives tumor-stroma co-evolution: A new paradigm for understanding tumor metabolism, the field effect and genomic instability in cancer cells. *Cell Cycle* 2010;9:3256–76.
34 Nolfi-Donegan D, Braganza A, Shiva S. Mitochondrial electron transport chain: Oxidative phosphorylation, oxidant production, and methods of measurement. *Redox Biol* 2020;37:101674.
35 Glorieux C, Liu S, Trachootham D, *et al*. Targeting ROS in cancer: rationale and strategies. *Nat Rev Drug Discov* 2024;23:583–606.
36 Shui X, Ren X, Xu R, *et al*. Monoamine oxidase A drives neuroendocrine differentiation in prostate cancer. *Biochem Biophys Res Commun* 2022;606:135–41.
37 Gross ME, Agus DB, Dorff TB, *et al*. Phase 2 trial of monoamine oxidase inhibitor phenelzine in biochemical recurrent prostate cancer. *Prostate Cancer Prostatic Dis* 2021;24:61–8.
38 Harper J, Sainson RCA. Regulation of the anti-tumour immune response by cancer-associated fibroblasts. *Semin Cancer Biol* 2014;25:69–77.
39 Ziani L, Chouaib S, Thiery J. Alteration of the Antitumor Immune Response by Cancer-Associated Fibroblasts. *Front Immunol* 2018;9:414.
40 Gok Yavuz B, Gunaydin G, Gedik ME, *et al*. Cancer associated fibroblasts sculpt tumour microenvironment by recruiting monocytes and inducing immunosuppressive PD-1^{+} TAMs. *Sci Rep* 2019;9:3172.
41 Takahashi H, Sakakura K, Kudo T, *et al*. Cancer-associated fibroblasts promote an immunosuppressive microenvironment through the induction and accumulation of protumoral macrophages. *Oncotarget* 2017;8:8633–47.
42 Chen Y, McAndrews KM, Kalluri R. Clinical and therapeutic relevance of cancer-associated fibroblasts. *Nat Rev Clin Oncol* 2021;18:792–804.
43 Bueno MLP, Saad STO, Roversi FM. WNT5A in tumor development and progression: A comprehensive review. *Biomed Pharmacother* 2022;155:113599.
44 Tufail M, Wu C. WNT5A: a double-edged sword in colorectal cancer progression. *Mutat Res Rev Mutat Res* 2023;792:108465.
45 Thiele S, Göbel A, Rachner TD, *et al*. WNT5A has anti-prostate cancer effects in vitro and reduces tumor growth in the skeleton in vivo. *J Bone Miner Res* 2015;30:471–80.